Generalized input-output method to quantum transport junctions. I. General formulation

Junjie Liu[1] and Dvira Segal[1,2]

[1]*Department of Chemistry and Centre for Quantum Information and Quantum Control, University of Toronto, 80 Saint George St., Toronto, Ontario, Canada M5S 3H6*

[2]*Department of Physics, 60 Saint George St., University of Toronto, Toronto, Ontario, Canada M5S 1A7*

(Received 25 November 2019; accepted 12 March 2020; published 6 April 2020)

The interaction of electrons with atomic motion critically influences charge transport properties in molecular conducting junctions and quantum dot systems, and it is responsible for a plethora of transport phenomena. Nevertheless, theoretical tools are still limited to treat simple model junctions in specific parameter regimes. In this paper, which forms the first paper of a series, we put forward a generalized input-output method (GIOM) for studying charge transport in molecular junctions accounting for strong electron-vibration interactions and including electronic and phononic environments. The method radically expands the scope of the input-output theory, which was originally put forward to treat quantum optic problems. Based on the GIOM, we derive a Langevin-type equation of motion for system operators, which possess a great generality and accuracy, and permits the derivation of a stationary charge current expression involving only two types of transfer rates. Furthermore, we devise the so-called polaron transport in electronic resonance approximation, which allows us to feasibly simulate electron dynamics in generic tight-binding models with strong electron-vibration interactions.

DOI: 10.1103/PhysRevB.101.155406

I. INTRODUCTION

Single-molecule devices offer a rich and versatile platform for exploring the fundamentals of charge and energy transport at the nanoscale and for making progress in electronic, photovoltaic, and thermoelectric systems [1]. A confounding aspect of electronic components fabricated from molecular building blocks is that they operate based on quantum mechanical principles, yet the surrounding environments in the form of electrical contacts, internal nuclear motion, solvent, and electromagnetic fields fundamentally impact and alter the charge-transport behavior. These environments do not fully erase quantum signatures in the device, but in fact allow for the realization of a plethora of compound many-body quantum transport effects that build upon hybrid quasi-particles, polarons, polaritons, and plasmons.

Efforts to utilize molecules as active electronic elements [2] have converged into the field of organic and molecular electronics [1]. Advanced experimental techniques [3–15] have led to the discovery of a variety of intriguing many-body phenomena in molecular junctions (MJs) in a metal-molecule-metal motif [16–19], including length and temperature-dependent charge transfer [12,13,20–35], quantum interference effects [14,36–40], molecular thermoelectricity [41–44], giant magnetoresistance [45], Kondo resonance [46,47], chirality induced spin selectivity [48–50], and Franck-Condon blockade (FCB) directed by vibrational effects [51–55], to name just a few.

The potential to rationally design molecular electronic devices hinges on our understanding of the underlying transport phenomena [19,40]. To this end, simplified theoretical models capable of pinpointing fundamental mechanisms are an indispensable tool. However, faithful modeling inevitably needs to take into account many-body interactions, specifically the coupling between electrons and the nuclei's motion. Moreover, the application of voltage bias on the contact electrodes necessitates a description of the junction in the out-of-equilibrium regime.

Numerous approaches have been put forward to address vibrationally coupled electron transport (VCET) processes in MJs and, similarly, quantum dot systems. A partial list of approximate analytic methods includes the inelastic scattering theory [56–61], which only accounts for coherent scattering events, mixed quantum-classical approaches [62–65] where the vibrations are treated in a classical-like fashion, quantum master equation (QME) techniques [66–77] which are often limited to weak molecule-lead couplings and become inadequate to describe off-resonant tunneling, and the nonequilibrium Green's function method (NEGF) [78–88]. Unambiguously, the NEGF is state of the art among these tools. However, its complicated structure limits its applicability to simple systems. Even so, standard formulations of the NEGF method can not account for strong electron-vibration interactions due to the cumulant expansion employed [89].

To provide benchmark calculations for analytic and perturbative studies, various numerically exact methods have been developed, among them the hierarchical equation of motion (HEOM) [90–98], multiconfigurational wave-function methods [99,100], path integral techniques based on Monte Carlo sampling [95,101–103], and the influence functional formalism [104–106]. Complementing model system calculations, first-principles density-functional theory simulations were integrated within the NEGF formalism [19,83,107–109] to include structural details of the junction and provide much insight into the transport process [19,40].

To make progress in organic and single-molecule electronics, it is imperative to develop a computationally feasible

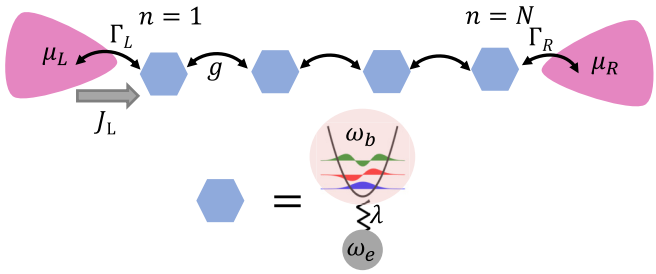

FIG. 1. Scheme of a metal-molecule-metal junction with N repeating molecular units. As a minimal model, each monomer (represented by a hexagon) includes a single electronic level of energy ω_e. The charge on each site is coupled to a local, "primary" vibrational mode of frequency ω_b, that is furthermore equilibrated by a thermal bath with "secondary" modes, represented by the shaded region surrounding the harmonic oscillator. Between monomers, g quantifies the charge-transfer transition amplitude. $\Gamma_{L,R}$ is the hybridization energy of the first and last sites to the left and right metal electrodes, respectively. Setting $\mu_L > \mu_R$, the main observable of interest is the steady-state charge current evaluated here at the left metal-molecule interface, J_L.

technique that treats (possibly strong) vibrational effects in electronic conduction and can handle extended models. In this first paper of a series, we tackle this challenge, introducing an alternative route to common QME and NEGF frameworks, tailored to the investigation of electron transport in molecular transport junctions. Our approach builds upon the quantum optical input-output method, which was previously advanced mainly for optical cavities [110–120]. The framework is termed the generalized input-output method (GIOM), and it possesses a simple structure—and a wide domain of applicability.

The GIOM relies on the definitions of generalized input and output fields for the environments, which circumvent the state-independent coupling approximation adopted in the quantum optical input-output theory [110,111,113]. Furthermore, the standard input-output theory is generalized here to include the coupling of system (molecular) operators to different (bosonic, fermionic) environmental degrees of freedom. Altogether, these extensions result in a so-called Heisenberg-Langevin equation (HLE) for molecular operators that takes into account strong couplings of the molecule to the metal electrodes as well as to vibrational modes, which comprise primary and secondary vibrations.

The appealing features of the GIOM are apparent in a generic tight-binding model describing VCET across molecules, quantum dots, and atoms, schematically represented in Fig. 1. In this case, HLEs for the electronic degrees of freedom permit a formally exact steady-state solution for the Hamiltonian we consider, which is amenable to approximations and simulations. Remarkably, the mathematically formal solution reveals that stationary charge current involves only two types of generalized transfer rates. To achieve a closed-form expression for the stationary charge current, we devise the polaron transport in electronic resonance (PoTER) approximation. The resulting charge current can be readily evaluated and becomes exact in the coherent limit, regardless of molecular complexities. Given this simplicity, the GIOM-PoTER framework can be readily implemented in large systems, thereby holding promise to bridge microscopic-oriented modelings and effective phenomenological descriptions. In the companion paper [121], we demonstrate the utility of the GIOM-PoTER scheme by investigating several prototypical MJ models.

The paper is organized as follows. We present the GIOM for generic VCET models in Sec. II. In Sec. III, we focus on a generic tight-binding model. We devise the PoTER approximation scheme, and derive a computationally feasible charge current expression in the steady-state limit. We summarize our work in Sec. IV.

II. GENERALIZED INPUT-OUTPUT METHOD

A. Quantum transport model

We start by defining a general model for describing VCET in MJs. The total Hamiltonian contains three different parts:

$$H = H_M + H_E + H_I. \tag{1}$$

First, the molecular Hamiltonian H_M accounts for a collection of electronic states with on-site energies $\{\omega_{e,n}\}$ and fermionic annihilation operators $\{d_n\}$, local molecular vibrations with frequencies $\{\omega_{b,n}\}$ and bosonic annihilation operators $\{b_n\}$, and electron-vibration couplings as measured by dimensionless coupling strengths $\{\lambda_n\}$ (setting $\hbar = 1$, $e = 1$, $k_B = 1$ and the Fermi energy $\epsilon_F = 0$ hereafter):

$$H_M = H_e(\{\omega_{e,n}, d_n\}) + \sum_n \omega_{b,n} b_n^\dagger b_n + \sum_n \lambda_n \omega_{b,n} (b_n^\dagger + b_n) d_n^\dagger d_n. \tag{2}$$

Here, we consider the coupling of each electronic site to a single local vibrational mode. However, generalizations to include additional vibrational modes per site, even yet creating a "bath" of primary modes, is straightforward within our scheme. Noting that the electronic part H_e may also depend on additional internal parameters, for the moment, however, its detailed form is not relevant and we do not specify it.

The environmental part H_E contains two metallic leads (L and R) and thermalized phonon baths that are associated with the local nuclear motions of molecules. These secondary modes allow vibrational relaxation of the primary modes:

$$H_E = \sum_{k,v=L,R} \epsilon_{kv} c_{kv}^\dagger c_{kv} + \sum_{n,j} \omega_{n,j} r_{n,j}^\dagger r_{n,j}. \tag{3}$$

Here c_{kv} annihilates an electron in lead v with momentum k. The thermal phonon baths are represented by collections of harmonic oscillators with annihilation operators $r_{n,j}$ and frequencies $\omega_{n,j}$. The third part, H_I, stands for the interaction between the molecule and its electronic and vibrational environments,

$$H_I = \sum_{k,v=L,R} t_{kv} (c_{kv}^\dagger d_\sigma + d_\sigma^\dagger c_{kv}) + \sum_{n,j} \gamma_{n,j} (r_{n,j}^\dagger b_n + b_n^\dagger r_{n,j}), \tag{4}$$

here, $\sigma = 1(N)$ for $v = L(R)$. We refer to d_σ as boundary operators since they are associated with terminal electronic

sites of the molecule. We assume that the interaction between the primary vibrational modes and the secondary-thermalized modes is rather weak such that the rotating wave approximation is justified. The influence of each thermal bath, acting on subunit n, is characterized by the spectral density $\nu_n(\omega) = \pi \sum_j \gamma_{n,j}^2 \delta(\omega - \omega_{n,j})$. Similarly, we introduce spectral densities for the metal leads as $\Gamma_v(\epsilon) = \pi \sum_k t_{kv}^2 \delta(\epsilon - \epsilon_{kv})$.

To handle potentially strong electron-vibration couplings, we perform the small polaron transformation with the unitary operator $G \equiv \prod_n (\mathcal{D}_{n,b})^{d_n^\dagger d_n}$ and displacement operators:

$$\mathcal{D}_{n,b} \equiv \exp[\lambda_n (b_n^\dagger - b_n)]. \tag{5}$$

We neglect the effect of this transformation on the coupling of primary modes to the thermal bath [80]. In more detail: In the polaron-transformed Hamiltonian, we ignore the effective weak interaction that forms between charge carriers and secondary phonons, $\sum_{n,j} \gamma_{n,j} \lambda_n d_n^\dagger d_n (r_{n,j}^\dagger + r_{n,j})$. This omission is justified in the present paper since the energy $\gamma_{n,j}\lambda_n$ is much smaller than electronic energies $\omega_{e,n}$ and the cutoff frequencies of the secondary bath, by noting that (in the Markov limit used) $\gamma_{n,j} \sim \sqrt{\nu_n}$ and $\nu \sim 10^{-3}$ eV in our calculations. The transformed Hamiltonian then reads

$$\tilde{H} = GHG^\dagger = \tilde{H}_M + H_E + \tilde{H}_I, \tag{6}$$

with

$$\tilde{H}_M = \tilde{H}_e(\{\tilde{\omega}_{e,n}, \tilde{d}_n\}) + \sum_n \omega_{b,n} b_n^\dagger b_n,$$

$$\tilde{H}_I = \sum_{kv} t_{kv}(c_{kv}^\dagger \tilde{d}_\sigma + \tilde{d}_\sigma^\dagger c_{kv}) + \sum_{n,j} \gamma_{n,j}(r_{n,j}^\dagger b_n + b_n^\dagger r_{n,j}). \tag{7}$$

As can be seen, the transformation amounts to the renormalization of on-site energies, $\omega_{e,n} \to \tilde{\omega}_{e,n} = \omega_{e,n} - \lambda_n^2 \omega_{b,n}$, and the dressing of the tunneling transition amplitudes; in the above expressions, we introduce the polaron operator as

$$\tilde{d}_n \equiv \mathcal{D}_{n,b}^\dagger d_n. \tag{8}$$

Before presenting the GIOM, we point out that while we discuss the model, the theoretical framework and our results in the context of molecular transport junctions, this work can be immediately applied to investigate related problems such as (i) Charge transport in quantum dot setups defined e.g., within nanotubes, with electrons coupled to different phonon modes of the nanotube [53,122] and (ii) quantum optics scenarios with quantum dots defined within heterostructures coupled to cavity modes and phonons of the substrate [123].

B. Input-output equations of motion

To develop an input-output theory for the system, we first write down Heisenberg equations of motion (EOMs) for the annihilation operators of the environments (electronic and secondary phonon modes) in the polaron frame,

$$\dot{r}_{n,j} = -i\omega_{n,j} r_{n,j} - i\gamma_{n,j} b_n, \tag{9a}$$

$$\dot{c}_{kv} = -i\epsilon_{kv} c_{kv} - i t_{kv} \tilde{d}_\sigma, \tag{9b}$$

where we have introduced the notation $\dot{A} \equiv dA/dt$. From the above EOMs, we get the following formal solutions:

$$r_{n,j}(t) = e^{-i\omega_{n,j}(t-t_0)} r_{n,j}(t_0) - i\gamma_{n,j} \int_{t_0}^{t} e^{-i\omega_{n,j}(t-\tau)} b_n(\tau) d\tau, \tag{10a}$$

$$c_{kv}(t) = e^{-i\epsilon_{kv}(t-t_0)} c_{kv}(t_0) - i t_{kv} \int_{t_0}^{t} e^{-i\epsilon_{kv}(t-\tau)} \tilde{d}_\sigma(\tau) d\tau. \tag{10b}$$

Here t_0 is the initial time at which the dynamical evolution begins. As the coupling of primary modes to the phonon thermal bath is weak, we approximate $b_n(\tau)$ by $b_n(t) e^{i\omega_{b,n}(t-\tau)}$ in Eq. (10a), yielding

$$\sum_j \gamma_{n,j} r_{n,j}(t) = \sqrt{2\pi} b_{in}^n(t) - i b_n(t) \sum_j \gamma_{n,j}^2 \times \int_{t_0}^{t} e^{-i(\omega_{n,j} - \omega_{b,n})(t-\tau)} d\tau, \tag{11}$$

where we have defined the input field:

$$b_{in}^n(t) \equiv \frac{1}{\sqrt{2\pi}} \sum_j \gamma_{n,j} e^{-i\omega_{n,j}(t-t_0)} r_{n,j}(t_0). \tag{12}$$

Assuming that $\nu_n(\omega)$ is about a constant at the vicinity of $\omega_{b,n}$, we find that $\sum_j \gamma_{n,j}^2 e^{-i(\omega_{n,j} - \omega_{b,n})t}$ is nonzero only around $t = 0$. We then extend the lower limit of integration on the right-hand side of Eq. (11) to $-\infty$ and proceed as $\sum_j \gamma_{n,j}^2 \int_0^\infty e^{-i(\omega_{n,j} - \omega_{b,n})\tau} d\tau \approx \nu_n(\omega_{b,n}) \equiv \nu_n$; we have neglected the Cauchy principal value, which just stands for a minute frequency renormalization. Overall, we get

$$\sum_j \gamma_{n,j} r_{n,j}(t) = \sqrt{2\pi} b_{in}^n(t) - i\nu_n b_n(t). \tag{13}$$

Here, ν_n is the damping rate (energy over $\hbar$) on site n of primary modes of frequency $\omega_{b,n}$ to the associated thermal bath. Contrasting this derivation to steps in the quantum optical input-output theory [110,111,113], we note that here we define the input field from the summation $\sum_j \gamma_{n,j} r_{n,j}$, instead of $\sum_j r_{n,j}$. By doing so, we circumvent the state-independent coupling approximation adopted in the quantum optical input-output theory [110,111,113], which assumes that the coupling coefficients $\gamma_{n,j} = \gamma_n$ are independent of the mode index j.

Proceeding with the metallic leads, we consider the wide-band limit [124] such that we can exactly turn Eq. (10b) into

$$\sum_k t_{kv} c_{kv}(t) = \sqrt{2\pi} d_{in}^v(t) - i\Gamma_v \tilde{d}_\sigma(t) \tag{14}$$

without compromising the magnitude of hybridization energy Γ_v. The input fields from the metal leads are defined as

$$d_{in}^v(t) \equiv \frac{1}{\sqrt{2\pi}} \sum_k t_{kv} e^{-i\epsilon_{kv}(t-t_0)} c_{kv}(t_0). \tag{15}$$

The definitions of input fields in terms of environment operators at the initial time ensure that they can be specified as initial conditions. Here, we prepare the initial state of the composite system to be such that, at $t = t_0$, the

molecule and its environments factorize. Specifically, we assume that the metal leads and the vibrational thermal baths are initially in their thermal equilibrium states characterized by the Fermi-Dirac distribution function $n_F^v(\epsilon) = \{\exp[(\epsilon-\mu_v)/T]+1\}^{-1}$ with μ_v the chemical potentials and T the temperature, and the Bose-Einstein distribution function $n_B(\omega) = [\exp(\omega/T)-1]^{-1}$, respectively. The resulting anticommutation/commutation relations, correlation functions for input fields, which define their statistics, as well as input-output relations that connect input and output fields can be found in Appendix A.

We now write down the Heisenberg EOM for an arbitrary molecular operator $\mathcal{O}$:

$$\dot{\mathcal{O}} = i[\tilde{H}_M, \mathcal{O}] - i\sum_{kv} t_{kv}\{[\mathcal{O}, c_{kv}^\dagger \tilde{d}_\sigma] + [\mathcal{O}, \tilde{d}_\sigma^\dagger c_{kv}]\} - i\sum_{n,j}\gamma_{n,j}\{[\mathcal{O}, r_{n,j}^\dagger b_n] + [\mathcal{O}, b_n^\dagger r_{n,j}]\}. \tag{16}$$

As the molecular system contains both fermionic and bosonic operators, we should treat them separately. To this end, we redefine quantum commutator and anticommutator as $[A,B]_- \equiv [A,B]$ and $[A,B]_+ \equiv \{A,B\}$, respectively. The EOM for $\mathcal{O}$ can be expressed as

$$\dot{\mathcal{O}} = i[\tilde{H}_M, \mathcal{O}]_- - i\sum_{kv} t_{kv}\{\mp c_{kv}^\dagger [\mathcal{O}, \tilde{d}_\sigma]_\pm + [\mathcal{O}, \tilde{d}_\sigma^\dagger]_\pm c_{kv}\} - i\sum_{n,j}\gamma_{n,j}\{r_{n,j}^\dagger [\mathcal{O}, b_n]_- + [\mathcal{O}, b_n^\dagger]_- r_{n,j}\}. \tag{17}$$

Here, the top signs apply if $\mathcal{O}$ is a fermionic operator; the bottom signs apply if $\mathcal{O}$ is bosonic. Making use of Eqs. (13) and (14), we obtain the HLE

$$\dot{\mathcal{O}} = i[\tilde{H}_M, \mathcal{O}]_- - i\sum_v \mathbb{L}_\pm^v - i\sum_n \mathbb{X}_n, \tag{18}$$

where the fermionic and bosonic environments enter through

$$\begin{aligned}\mathbb{L}_\pm^v &\equiv \mp\big(i\Gamma_v \tilde{d}_\sigma^\dagger + \sqrt{2\pi} d_{in}^{v,\dagger}\big)[\mathcal{O}, \tilde{d}_\sigma]_\pm \\ &\quad + [\mathcal{O}, \tilde{d}_\sigma^\dagger]_\pm\big(-i\Gamma_v \tilde{d}_\sigma + \sqrt{2\pi} d_{in}^v\big), \\ \mathbb{X}_n &\equiv \big(i\nu_n b_n^\dagger + \sqrt{2\pi} b_{in}^{n,\dagger}\big)[\mathcal{O}, b_n]_- \\ &\quad + [\mathcal{O}, b_n^\dagger]_-\big(-i\nu_n b_n + \sqrt{2\pi} b_{in}^n\big).\end{aligned} \tag{19}$$

This HLE constitutes the first main result of this study. Before proceeding to derive it for tight-binding models, there are several features of Eq. (18) that are worth mentioning. First, it does not rely on molecular details and thus possesses a great generality. Second, the electronic part is treated exactly in the wide band limit. Third, there is no corresponding Lindblad master equation for Eq. (18) as it can treat possible strong hybridization energy, in direct contrast to standard quantum optical input-output theory [111]. Moreover, the equation conserves the overall charge.

The main observable of interest in the steady-state limit is the charge current across the system. Introducing the charge occupation number operator of the left lead (source electrode), $n_L \equiv \sum_k c_{kL}^\dagger c_{kL}$, the charge current out of the L metal is formally given by

$$J_L = -\frac{d}{dt}\langle n_L\rangle = i\sum_k t_{kL}\langle (c_{kL}^\dagger \tilde{d}_1 - \tilde{d}_1^\dagger c_{kL})\rangle, \tag{20}$$

with the average performed over the initial factorized state of the composite system. In the language of the input field, using Eq. (14), we get

$$J_L = 2\big(\sqrt{2\pi}\,\mathrm{Im}\langle \tilde{d}_1^\dagger d_{in}^L\rangle - \Gamma_L\langle d_1^\dagger d_1\rangle\big). \tag{21}$$

Here, Im refers to an imaginary part.

In a complete analogy to the input fields, one can define output fields by solving Eqs. (9a) and (9b) for $t_1 > t$, rather than from the initial condition t_0 (see Appendix A). This allows the derivation of a Langevin-type equation, which is parallel to Eq. (18), but given in terms of the output fields. However, due to the existence of input-output relations as given in Appendix A, it is sufficient to work with the input fields.

Before proceeding, we recall other EOM methods that have been developed to treat transport problems, such as the Heisenberg EOM approach [125,126] and methods written in the form of the Langevin equation [63,127]. However, so far, the Heisenberg EOM approach has been only applied to simple noninteracting electronic systems, since it requires the inverse Laplace transform to calculate the dynamics of observables, typically a tedious and prohibitive task in molecular systems. Langevin equation techniques discussed in the literature for quantum transport are formulated for density matrix elements within the scope of the QME [63,127]. In contrast, the GIOM formulates the dynamics at the level of operators, rather than states, and it is nonperturbative.

III. GIOM FOR TIGHT-BINDING MODELS

We now apply the HLE Eq. (18) to a generic tight-binding model with electron-vibration couplings, culminating with a closed-form expression for the stationary charge current. The section includes two powerful results of theoretical and computational importance:

(i) From the theoretical side, we arrive at a formally exact EOM, Eq. (24), for molecular electronic operators in an open, many-body system described by the polaronic Hamiltonian [cf. Eq. (6) together with Eq. (22)], barring two elements from our modeling: The effective electron-secondary phonon bath coupling was omitted from the polaronic Hamiltonian, and the wide band limit for the reservoirs was enforced. One can write down a formal solution to Eq. (24), that is, Eq. (29). However, we point out that Eq. (29) is not closed, in the sense that it should be supplemented by EOMs for the local vibrations. Nevertheless, Eq. (29) already leads to an interesting fundamental observation that the functional form of the stationary charge current only depends on two kinds of transfer rates involving one or two electronic resonances.

(ii) To allow feasible calculations, we further devise an approximate solution to Eq. (24), that is, Eq. (32). This solution neglects some aspects of electron-vibration interactions (as we describe in this section), and we refer to it as the PoTER approximation. As evident from its title, this PoTER approximation describes the transport of polarons through

electronic resonances, eigenstates of electronic Hamiltonian H_e that are broadened by their hybridization to the metal reservoirs. Notably, in the context of the GIOM, the electronic current is given in terms of only two types of rates, and the PoTER approximation allows for an economical simulation of these rates, and therefore the charge current for a broad range of parameters.

A. Formally exact dynamical solution for electrons

We specify the model Hamiltonian of Eqs. (6) and (7) and apply the GIOM. The model includes a tight-binding chain with vibrational coupling, see Fig. 1. We assign a single electronic state to each repeat unit of a molecular wire. For the electronic part, we therefore have

$$\tilde{H}_e = \sum_{n=1}^{N} \tilde{\omega}_{e,n} d_n^\dagger d_n + \sum_{n=1}^{N-1} g_n (\tilde{d}_n^\dagger \tilde{d}_{n+1} + \tilde{d}_{n+1}^\dagger \tilde{d}_n), \tag{22}$$

with g_n as the hopping element between sites n and $n+1$; N is the total number of electronic states. The single-site case, $N=1$, corresponds to the eminent single-impurity Anderson-Holstein model. Multisite extensions involve two electronic sites, and beyond.

Inserting the above form into Eq. (18), we obtain the following coupled EOMs for the bare electronic operators d_n,

$$\begin{aligned}
\dot{d}_1 &= -(\Gamma_L + i\tilde{\omega}_{e,1}) d_1 - i g_1 \mathcal{D}_{1,b} \mathcal{D}_{2,b}^\dagger d_2 - i\sqrt{2\pi}\mathcal{D}_{1,b} d_{in}^L, \\
\dot{d}_{n\neq 1,N} &= -i\tilde{\omega}_{e,n} d_n - i g_{n-1} \mathcal{D}_{n,b} \mathcal{D}_{n-1,b}^\dagger d_{n-1} \\
&\quad - i g_n \mathcal{D}_{n,b} \mathcal{D}_{n+1,b}^\dagger d_{n+1}, \\
\dot{d}_N &= -(\Gamma_R + i\tilde{\omega}_{e,N}) d_N - i g_{N-1} \mathcal{D}_{N,b} \mathcal{D}_{N-1,b}^\dagger d_{N-1} \\
&\quad - i\sqrt{2\pi}\mathcal{D}_{N,b} d_{in}^R.
\end{aligned} \tag{23}$$

Notably, EOMs for boundary operators $d_{1,N}$ naturally incorporate level broadening due to molecule-lead coupling. By introducing column vectors $\boldsymbol{d} = (d_1, d_2, \cdots, d_N)^T$, $\tilde{\boldsymbol{d}}_{in} = (\mathcal{D}_{1,b} d_{in}^L, 0, \cdots, 0, \mathcal{D}_{N,b} d_{in}^R)^T$, we recast Eqs. (23) into a matrix form:

$$\dot{\boldsymbol{d}} = -\boldsymbol{M} \cdot \boldsymbol{d} - i\sqrt{2\pi}\tilde{\boldsymbol{d}}_{in}. \tag{24}$$

Note that $\tilde{\boldsymbol{d}}_{in}$ includes the dressing of input fields by displacement operators. The drift matrix $\boldsymbol{M}$ is of a tridiagonal structure with elements $[\boldsymbol{M}]_{nm} = W_{nm}\mathcal{D}_{n,b}\mathcal{D}_{m,b}^\dagger$. Here, $W_{nn} = \Gamma_L \delta_{n1} + \Gamma_R \delta_{nN} + i\tilde{\omega}_{e,n}$ and $W_{n,n+1} = W_{n+1,n} = i g_n$; δ_{kp} is the Kronecker delta function.

We now formally introduce the matrix $\boldsymbol{R}$ whose rows are made of the left eigenvectors of the drift matrix $\boldsymbol{M}$:

$$\boldsymbol{R} \cdot \boldsymbol{M} = \boldsymbol{\Lambda}_M \cdot \boldsymbol{R}. \tag{25}$$

Here $\boldsymbol{\Lambda}_M = \mathrm{diag}(\Lambda_1, \cdots, \Lambda_N)$ is a diagonal matrix with eigenvalues $\{\Lambda_n\}$ representing electronic resonances. The fact that electronic resonances are characterized by complex c numbers implies the form for matrix elements in the site basis, $[\boldsymbol{R}]_{nm} = \tilde{s}_{nm}\mathcal{D}_{n,b}\mathcal{D}_{m,b}^\dagger$ with $\tilde{s}_{nm}$ complex c numbers according to Eq. (25).

We now make an important observation: The determinant of $\boldsymbol{M} - \Lambda \boldsymbol{I}$ is equivalent to that of another tridiagonal matrix, $\boldsymbol{M_0} - \Lambda \boldsymbol{I}$, having the same eigenvalue matrix Λ and $[\boldsymbol{M_0}]_{nm} = W_{nm}$; the $\boldsymbol{M_0}$ matrix does not include vibrational operators.

This claim can be proved by noting that the determinant of a tridiagonal matrix can be easily evaluated through the continuant of its elements. Defining $f_N = \det[\boldsymbol{M}_{N\times N} - \Lambda \boldsymbol{I}_{N\times N}]$, the sequence $\{f_N\}$ is called the continuant and satisfies the recurrence relation $f_N = (W_{NN} - \Lambda) f_{N-1} + g_{N-1}^2 f_{N-2}$ with the boundary conditions $f_1 = \Gamma_L + i\tilde{\omega}_{e,1} - \Lambda$, $f_0 = 1$ and $f_{-1} = 0$. As can be seen, the sequence is fully equivalent to that of $\boldsymbol{M_0} - \Lambda \boldsymbol{I}$. Therefore, the task of determining $\boldsymbol{R}$ and $\boldsymbol{\Lambda}_M$ corresponds to the diagonalization problem of $\boldsymbol{R_0} \cdot \boldsymbol{M_0} = \boldsymbol{\Lambda}_M \cdot \boldsymbol{R_0}$ with $[\boldsymbol{R_0}]_{nm} = \tilde{s}_{nm}$, thereby avoiding the displacement operators that appear in the original matrices. In fact, this correspondence also holds for one-dimensional models with long-range interactions, noting that displacement operators involved in $[\boldsymbol{M}]_{nm}$ and $[\boldsymbol{M}]_{mn}$ are always complex conjugate.

For small N, this diagonalization permits an analytical treatment. For larger N, we resort to a numerical diagonalization of the tridiagonal matrix $\boldsymbol{M_0}$. We reiterate that the diagonal matrix $\boldsymbol{\Lambda}_M$ involves the set of electronic resonances of the system (c numbers). These broadened energy levels describe the electronic states of a molecule hybridized to metal electrodes. Equipped with the knowledge that the diagonal matrix $\boldsymbol{\Lambda}_M$ does not depend on nuclear coordinates, we rewrite Eq. (24):

$$\boldsymbol{R} \cdot \dot{\boldsymbol{d}} = -\boldsymbol{\Lambda}_M \cdot \boldsymbol{R} \cdot \boldsymbol{d} - i\sqrt{2\pi}\boldsymbol{R} \cdot \tilde{\boldsymbol{d}}_{in}. \tag{26}$$

To proceed, we further reorganize Eq. (26):

$$\frac{d}{dt}(\boldsymbol{R} \cdot \boldsymbol{d}) = -(\boldsymbol{\Lambda}_M - \dot{\boldsymbol{R}} \cdot \boldsymbol{R}^{-1}) \cdot \boldsymbol{R} \cdot \boldsymbol{d} - i\sqrt{2\pi}\boldsymbol{R} \cdot \tilde{\boldsymbol{d}}_{in}. \tag{27}$$

Here, $\boldsymbol{R}^{-1}$ denotes the inverse matrix of $\boldsymbol{R}$ with the matrix elements $[\boldsymbol{R}^{-1}]_{nm} = s_{nm}\mathcal{D}_{n,b}\mathcal{D}_{m,b}^\dagger$. Unlike $\boldsymbol{\Lambda}_M$, $\dot{\boldsymbol{R}} \cdot \boldsymbol{R}^{-1}$ depends on the nuclear coordinates, and it includes nonzero off-diagonal matrix elements in the site basis:

$$\begin{aligned}
[\dot{\boldsymbol{R}} \cdot \boldsymbol{R}^{-1}]_{nm} &= \sum_k \tilde{s}_{nk} s_{km} (\lambda_n \dot{P}_n - \lambda_k \dot{P}_k) \mathcal{D}_{n,b}\mathcal{D}_{m,b}^\dagger \\
&= \delta_{nm}\lambda_n \dot{P}_n - \sum_k \tilde{s}_{nk} s_{km} \lambda_k \dot{P}_k \mathcal{D}_{n,b}\mathcal{D}_{m,b}^\dagger.
\end{aligned} \tag{28}$$

For simplicity, we introduce the notation $P_n \equiv b_n^\dagger - b_n$. In obtaining the second line, we used the fact that $\sum_k \tilde{s}_{nk} s_{km} \mathcal{D}_{n,b}\mathcal{D}_{m,b}^\dagger = \delta_{nm}$ since $\boldsymbol{R} \cdot \boldsymbol{R}^{-1} = \boldsymbol{I}$.

The exact dynamical evolution of electronic degrees of freedom is given by the formal solution of Eq. (27) in the steady-state limit:

$$\begin{aligned}
\boldsymbol{d}(t) = -i\sqrt{2\pi} \int_{-\infty}^{t} d\tau \boldsymbol{R}^{-1}(t) e^{-\boldsymbol{\Lambda}_M (t-\tau)} \\
\times e^{\int_\tau^t \dot{\boldsymbol{R}}(\tau')\boldsymbol{R}^{-1}(\tau') d\tau'} \boldsymbol{R}(\tau) \tilde{\boldsymbol{d}}_{in}(\tau).
\end{aligned} \tag{29}$$

The term resulting from the initial condition, $\boldsymbol{d}(t_0)$, is dropped as it does not contribute to the ensemble average in the steady-state limit [for the terms involved in charge current Eq. (21), this is evident by noting the causality that $\boldsymbol{d}(t_0)$ does not correlate with the input fields in the future].

From the above formal solution, we can find, for instance, the evolution of the operator d_1,

$$d_1(t) = -i\sqrt{2\pi}\sum_{nm}\int_{-\infty}^{t} d\tau\big[s_{1n}\tilde{s}_{m1}K_{nm}(t,\tau)d_{in}^{L}(\tau) + s_{1n}\tilde{s}_{mN}K_{nm}(t,\tau)d_{in}^{R}(\tau)\big], \tag{30}$$

where we defined

$$K_{nm}(t,\tau) = e^{-\Lambda_n(t-\tau)}\mathcal{D}_{1,b}(t)\mathcal{D}_{n,b}^{\dagger}(t) \times\left[\exp\left(\int_{\tau}^{t}(\dot{\boldsymbol{R}}\boldsymbol{R}^{-1})_{\tau'}d\tau'\right)\right]_{nm}\mathcal{D}_{m,b}(\tau). \tag{31}$$

This term incorporates all the vibrational effects. Altogether, beginning with the exact EOM of the GIOM, Eq. (24), we obtain a formally exact solution Eq. (29) for electronic operators. Interestingly, by inserting Eq. (30) into Eq. (21), one immediately reveals that the charge current expression builds upon only two types of transfer processes involving one and two electronic resonances, which we will elaborate on later. Nevertheless, since nuclear coordinates appear in the combination $(\dot{\boldsymbol{R}}\boldsymbol{R}^{-1})_{\tau'}$, which evolves in time according to the full Hamiltonian $\tilde{H}$ given by Eq. (6), the problem is formidable and it requires making approximations to become practical.

B. PoTER approximation

We now devise an approximation that allows us to reach a highly efficient computational scheme for solving the GIOM equations, Eq. (24), and obtain a closed form for stationary charge current. This so-called PoTER approximation includes two components. In Sec. III B 1, we elaborate on the first part of the PoTER approximation: polarons are transmitted between the metals through purely electronic resonances. In Sec. III B 2, we perform the second part of the PoTER approximation: The vibrational degrees of freedom, which form the polaron, time evolve without the back action of electrons.

1. First part of PoTER: Simplified dynamical evolution

Under the first part of the PoTER approximation, we simplify the kernel in Eq. (31) and replace $[\exp(\int_{\tau}^{t}(\dot{\boldsymbol{R}}\boldsymbol{R}^{-1})_{\tau'}d\tau')]_{nm}$ with δ_{nm}. This approximation amounts to (i) neglecting nonlocal vibration effects with $n \neq m$ in the dynamical evolution of electronic degrees of freedom and (ii) neglecting phonon corrections to the electronic resonances. This reduces Eq. (29) to

$$\boldsymbol{d}(t) \approx -i\sqrt{2\pi}\int_{-\infty}^{t} d\tau\boldsymbol{R}^{-1}(t)e^{-\boldsymbol{\Lambda}_M(t-\tau)}\boldsymbol{R}(\tau)\tilde{\boldsymbol{d}}_{in}(\tau). \tag{32}$$

Specifically, Eq. (30) becomes

$$d_1(t) \approx -i\sqrt{2\pi}\sum_{n}\int_{-\infty}^{t} d\tau\big[s_{1n}\tilde{s}_{n1}K_{n}^{\mathrm{PoTER}}(t,\tau)d_{in}^{L}(\tau) + s_{1n}\tilde{s}_{nN}K_{n}^{\mathrm{PoTER}}(t,\tau)d_{in}^{R}(\tau)\big], \tag{33}$$

with the PoTER kernel,

$$K_{n}^{\mathrm{PoTER}}(t,\tau) = e^{-\Lambda_n(t-\tau)}\mathcal{D}_{1,b}(t)\mathcal{D}_{n,b}^{\dagger}(t)\mathcal{D}_{n,b}(\tau). \tag{34}$$

For simplicity, in what follows we replace the approximate symbol by an equality, since we consistently work the PoTER approximation.

Elaborating on this approximation, the term $(\dot{\boldsymbol{R}}\boldsymbol{R}^{-1})$ in Eq. (29) involves time derivative of $\mathcal{D}_{n,b}\mathcal{D}_{m,b}^{\dagger}$. It is proportional to $\lambda_n\dot{P}_n - \lambda_m\dot{P}_m$, or approximately to $\lambda_n\omega_{b,n}(b_n^{\dagger}+b_n) - \lambda_m\omega_{b,m}(b_m^{\dagger}+b_m)$, once we consider free vibrations, $b_n^{\dagger}(t) = b_n^{\dagger}(0)e^{i\omega_{b,n}t}$. Therefore, the first part of the PoTER approximation amounts to assuming that nuclear displacements are uniform across the lattice. This assumption is expected to be reasonably valid for a tight-binding model with identical (or similar) repeating units and when the dissipation to secondary modes is weak.

It is worth mentioning that (i) the PoTER solution Eq. (32) is exact in the coherent limit ($\{\lambda_n\} \to 0$) since then $\boldsymbol{R}$ is strictly time independent, (ii) in Appendix B, we prove that the PoTER scheme does not impact the total charge conservation, and (iii) the solution for $d_1^{\dagger}$ is just the Hermitian transpose of Eq. (33); the PoTER approximation does not cripple this relation. We show that by writing down the EOM for row vectors $\boldsymbol{d}^{\dagger} = (d_1^{\dagger}, d_2^{\dagger}, \cdots, d_N^{\dagger})$, $\tilde{\boldsymbol{d}}_{in}^{\dagger} = (d_{in}^{L,\dagger}\mathcal{D}_{1,b}^{\dagger}, 0, \cdots, 0, d_{in}^{R,\dagger}\mathcal{D}_{N,b}^{\dagger})$,

$$\dot{\boldsymbol{d}}^{\dagger} = -\boldsymbol{d}^{\dagger}\cdot\boldsymbol{M}^{\dagger} + i\sqrt{2\pi}\tilde{\boldsymbol{d}}_{in}^{\dagger}. \tag{35}$$

We diagonalize $\boldsymbol{M}^{\dagger}$ in terms of $\boldsymbol{M}^{\dagger}\cdot\boldsymbol{Q} = \boldsymbol{Q}\cdot\boldsymbol{\Lambda}_M^{\star}$ with $\boldsymbol{Q} = \boldsymbol{R}^{\dagger}$ and find the PoTER solution $\boldsymbol{d}^{\dagger}(t) = i\sqrt{2\pi}\int_{-\infty}^{t} d\tau\tilde{\boldsymbol{d}}_{in}^{\dagger}(\tau)\boldsymbol{Q}(\tau)e^{-\boldsymbol{\Lambda}_M^{\star}(t-\tau)}\boldsymbol{Q}^{-1}(t)$, which is the Hermitian transpose of Eq. (32). Hence, we can obtain $d_1^{\dagger}$ directly from the Hermitian transpose of Eq. (33).

So far, we discussed the first part of the PoTER approximation: Polarons are transmitted through purely electronic resonances. The second part of the approximation is practiced in the next subsection and it concerns the time evolution of the vibrations forming the polaron: We propagate the displacement operators $\mathcal{D}_{n,b}(t)$ while ignoring back action from charge carriers. This approximation allows us to prepare and evaluate the time correlation function of the polaron, a component in the expression of the charge current.

2. Second part of PoTER: Charge current expression

In this section, we derive a closed-form expression for the steady-state charge current. Our starting point is the definition, Eq. (21), with the average performed with respect to the initial total density matrix, which is assumed to be in a factorized form, $\rho(t=0) = \rho_e \otimes \rho_b$. Here ρ_e is the initial state for the electronic degrees of freedom, factorized to the two baths and the molecular electronic system, $\rho_e = \rho_L \otimes \rho_R \otimes \rho_S$. ρ_b is the initial state for the bosonic modes. It is factorized between the N sites, and between the the primary and secondary modes, the latter are assumed to be in a thermal state.

Using the PoTER solution, Eq. (33), and the commutation relations of input fields from Appendix A, we get

$$\sqrt{2\pi}\mathrm{Im}\langle\tilde{d}_1^{\dagger}d_{in}^{L}\rangle = \sum_{n}\mathrm{Re}\big[\Phi_n^{L}\chi_n^{L}\big]. \tag{36}$$

Here Re refers to the real part. We have denoted by $\Phi_n^L = s_{1n}\tilde{s}_{n1}$ and defined the transfer rate

$$\chi_n^v = 2\Gamma_v \int \frac{d\epsilon}{2\pi} n_F^v(\epsilon) \int_0^\infty d\tau e^{i\epsilon\tau} e^{-\Lambda_n \tau} B_n(\tau), \tag{37}$$

with the vibrational correlation function $B_n(t-\tau) = \langle \mathcal{D}_{n,b}^\dagger(t)\mathcal{D}_{n,b}(\tau)\rangle$; the index n recounts the electronic resonances. We refer to this rate as first order since it involves a single electronic resonance, Λ_n. Clearly, χ_n^v describes a transfer event assisted by a single electronic resonance and dressed by local vibrational correlations.

The derivation of Eq. (37) is detailed in Appendix C. It involves the second part of the PoTER approximation: We ignore the back action of electrons on primary modes in the polaron frame and separately organize electronic and vibrational correlation functions. This step corresponds to the electron-vibration decoupling approximation implemented in NEGF-based studies [89].

We proceed and calculate the vibrational correlation function using the decoupled EOMs for the primary modes, Eq. (18), $\dot{b}_n \approx -(\nu_n + i\omega_{b,n})b_n - i\sqrt{2\pi}b_{in}^n$. We get

$$B_n(\tau) = \exp\left[-\lambda_n^2 \int d\omega \frac{\nu_n(\omega)}{\pi} \frac{1}{\nu_n^2 + (\omega-\omega_{b,n})^2} \times (\coth(\beta\omega/2)(1-\cos\omega\tau) + i\sin\omega\tau)\right]. \tag{38}$$

Details can be found in Appendix D.

The second contribution to the charge current involves the stationary charge occupation on the first site:

$$\langle d_1^\dagger d_1\rangle = \frac{1}{2}\sum_{nm,v} \frac{\Psi_{nm}^v}{\Gamma_v}\eta_{nm}^v. \tag{39}$$

Here, we have denoted the coefficients $\Psi_{nm}^L = s_{1n}^\star \tilde{s}_{n1}^\star s_{1m}\tilde{s}_{m1}$, $\Psi_{nm}^R = s_{1n}^\star \tilde{s}_{nN}^\star s_{1m}\tilde{s}_{mN}$ and introduced the transfer rate (see Appendix C):

$$\eta_{nm}^v = 4\Gamma_v^2 \int \frac{d\epsilon}{2\pi} n_F^v(\epsilon)\left[\int_0^\infty d\tau e^{i\epsilon\tau} e^{-\Lambda_n\tau} B_n(\tau)\right]^\star \times \left[\int_0^\infty d\tau e^{i\epsilon\tau} e^{-\Lambda_m\tau} B_m(\tau)\right]. \tag{40}$$

We refer to this rate as second order since it involves two resonances; diagonal terms are exceptions as they reduce to first-order rates, $\eta_{nn}^v = \frac{2\Gamma_v}{\mathrm{Re}\Lambda_n}\mathrm{Re}[\chi_n^v]$, after performing a time integration. To evaluate the autocorrelation function of the polaron, we neglect the back action of electrons on the vibrational dynamics.

Inserting Eqs. (36) and (39) into Eq. (21), we build the final expression for the charge current out of the left lead:

$$J_L = 2\sum_n \mathrm{Re}\left[\Phi_n^L \chi_n^L\right] - \Gamma_L \sum_{nm,v} \frac{\Psi_{nm}^v}{\Gamma_v}\eta_{nm}^v. \tag{41}$$

Similarly, the steady-state charge current out of the right lead, J_R, can be expressed as $J_R = 2\sum_n \mathrm{Re}[\Phi_n^R\chi_n^R] - \Gamma_R\sum_{nm,v}\frac{\tilde{\Psi}_{nm}^v}{\Gamma_v}\eta_{nm}^v$ with $\Phi_n^R = s_{Nn}\tilde{s}_{nN}$, $\tilde{\Psi}_{nm}^R = s_{Nn}^\star \tilde{s}_{nN}^\star s_{Nm}\tilde{s}_{mN}$ and $\tilde{\Psi}_{nm}^L = s_{Nn}^\star \tilde{s}_{n1}^\star s_{Nm}\tilde{s}_{m1}$. These two analytic charge current expressions represent one of main results of this study. As the method maintains the charge conservation, it should satisfy $J_L = -J_R$ in the steady-state limit.

Notably, the charge current involves only two types of rates as revealed by the GIOM, regardless of molecular complexities. The PoTER approximation allows their facile evaluation with computational efforts scaling quadratically with system size, N^2: The rates χ_n depend on individual eigenvalues Λ_n. The rates η_{nm} involve charge transfer jointly through two resonances.

C. Discussion

When do we expect the GIOM-PoTER treatment to be accurate? As mentioned above, the PoTER approximation does not affect the purely electronic problem, i.e., it exactly recovers the Landauer form with the correct transmission function. It is also expected to be accurate in the low-temperature regime when nuclear motion is largely suppressed. Moreover, for the single impurity problem *with* electron-vibration interaction, Eq. (32) is exact since $\boldsymbol{M}$ simply involves the electronic resonance without vibrational corrections, which are fully delegated to the input fields. In other words, the first part of the PoTER approximation is redundant for the single-site case. Lastly, for short wires, we expect corrections to Eq. (32) due to nonlocal vibrational effects and vibrational self-energies to be minor. However, these terms could become important in long wires, particularly once energy dissipation is substantial.

Before concluding, it it worthwhile to compare and contrast the PoTER scheme with existing approximations on electron-vibration coupling in quantum transport problems such as the Born-Oppenheimer adiabatic decoupling scheme [80], the polaron tunneling approximation [128], and the dressed tunneling approximation [129]. These methods, based on the nonequilibrium Green's function formulation, were described for the single-site case, for which the first PoTER approximation becomes redundant. The second part of PoTER is similar to approximations performed in NEGF-based studies. There, the electron-phonon decoupling approximation corresponds to neglecting parts of the electron-vibration correlations, as we do in the second PoTER approximation. However, in our paper, we do not invoke a self-consistent procedure, which can readmit parts of the neglected electron-phonon correlation. These corrections will be considered in future work.

IV. SUMMARY

In this work, we presented an original framework for studying the electronic current in vibrationally coupled MJs, an alternative approach to standard (often costly and cumbersome) nonequilibrium Green's function and perturbative QME methods. Specifically, there are two main contributions to this paper:

(i) The first achievement lies in the generalization of the quantum optical input-output method to treat quantum transport junction problems culminating with a formally exact electronic equation of motion [cf. Eq. (24)] for the polaronic Hamiltonian we considered. A central advantage of our GIOM lies in its transparency: The formal steady-state solution (at

the level of operators), Eq. (29), clearly displays the effect of electron-vibration couplings on electron transport: This interaction leads to the formation of polarons that are transported through vibrationally modified electronic resonances.

(ii) We devise an approximation scheme to the GIOM, that is, the PoTER solution. Equation (32) describes polaron transport through purely electronic resonances. Expectation values for electronic operators are calculated by neglecting nonlocal vibrational correlations as well as back actions of electrons on vibrations. Using this approach, we avoid perturbation expansions of parameters, achieve computationally manageable closed-form expressions for the charge current, and explore challenging parameter regimes. Notably, in the GIOM scheme, the charge current expression for a generic tight-binding model involves only two types of transfer rates, which are easily computed under the PoTER approximation.

In the companion paper to this one [121], we focus on applications of the GIOM-PoTER framework in paradigmatic MJs of tight-binding forms. This includes single-site and two-site models, which are frequently employed in experiment-theory studies, as well as cavity-coupled MJs.

ACKNOWLEDGMENTS

The authors acknowledge support from the Natural Sciences and Engineering Research Council (NSERC) of Canada Discovery Grant and the Canada Research Chairs Program. We also thank an anonymous referee for insightful comments.

APPENDIX A: STATISTICS OF INPUT FIELDS AND INPUT-OUTPUT RELATIONS

From the definitions of the input fields, we easily identify the following commutation/anticommutation relations:

$$\left[b_{in}^{n}(t), b_{in}^{m,\dagger}(t')\right] = \delta_{nm}\int d\omega \frac{\nu_n(\omega)}{2\pi^2} e^{-i\omega(t-t')}, \quad \text{(A1a)}$$

$$\left\{d_{in}^{v}(t), d_{in}^{v',\dagger}(t')\right\} = \delta_{vv'}\Gamma_v \int \frac{d\epsilon}{2\pi^2} e^{-i\epsilon(t-t')}, \quad \text{(A1b)}$$

from which we obtain the following correlation functions for input fields:

$$\begin{aligned}
\left\langle b_{in}^{n,\dagger}(t')b_{in}^{m}(t)\right\rangle &= \delta_{nm}\int d\omega \frac{\nu_n(\omega)}{2\pi^2} e^{-i\omega(t-t')} n_B(\omega),\\
\left\langle b_{in}^{n}(t)b_{in}^{m,\dagger}(t')\right\rangle &= \delta_{nm}\int d\omega \frac{\nu_n(\omega)}{2\pi^2} e^{-i\omega(t-t')}\left[1+n_B(\omega)\right],\\
\left\langle d_{in}^{v,\dagger}(t')d_{in}^{v'}(t)\right\rangle &= \delta_{vv'}\Gamma_v \int \frac{d\epsilon}{2\pi^2} e^{-i\epsilon(t-t')} n_F^v(\epsilon),\\
\left\langle d_{in}^{v}(t)d_{in}^{v',\dagger}(t')\right\rangle &= \delta_{vv'}\Gamma_v \int \frac{d\epsilon}{2\pi^2} e^{-i\epsilon(t-t')}\left[1-n_F^v(\epsilon)\right]. \quad \text{(A2)}
\end{aligned}$$

Here $n_B(\omega) = \{\exp[\omega/T]-1\}^{-1}$ and $n_F^v(\epsilon) = \{\exp[(\epsilon-\mu_v)/T]+1\}^{-1}$ are the Bose-Einstein distribution and the Fermi-Dirac distribution, respectively.

To define output fields, we express the formal solution of Eqs. (9a) and (9b) in terms of the final conditions $r_{n,j}(t_1)$ and $c_{kv}(t_1)$ at a later time $t_1 > t$:

$$r_{n,j}(t) = e^{-i\omega_{n,j}(t-t_1)} r_{n,j}(t_1) + i\gamma_{n,j}\int_t^{t_1} e^{-i\omega_{n,j}(t-\tau)} b_n(\tau)d\tau, \quad \text{(A3a)}$$

$$c_{kv}(t) = e^{-i\epsilon_{kv}(t-t_1)} c_{kv}(t_1) + it_{kv}\int_t^{t_1} e^{-i\epsilon_{kv}(t-\tau)}\tilde{d}_\sigma(\tau)d\tau. \quad \text{(A3b)}$$

Introducing output fields

$$b_{\rm out}^{n}(t) \equiv \frac{1}{\sqrt{2\pi}}\sum_j \gamma_{n,j} e^{-i\omega_{n,j}(t-t_1)} r_{n,j}(t_1), \quad \text{(A4a)}$$

$$d_{\rm out}^{v}(t) \equiv \frac{1}{\sqrt{2\pi}}\sum_k t_{kv} e^{-i\epsilon_{kv}(t-t_1)} c_{kv}(t_1), \quad \text{(A4b)}$$

we obtain the input-output relations,

$$b_{\rm out}^{n}(t) - b_{in}^{n}(t) = -i\sqrt{\frac{2}{\pi}}\nu_n b_n(t), \quad \text{(A5a)}$$

$$d_{\rm out}^{v}(t) - d_{in}^{v}(t) = -i\sqrt{\frac{2}{\pi}}\Gamma_v \tilde{d}_\sigma(t). \quad \text{(A5b)}$$

APPENDIX B: CHARGE CONSERVATION

The total charge should be conserved in the junction, that is in the molecule + metals. Given the approximate solution, Eq. (32), its validity in this respect requires a careful examination. To this end, we focus on the time derivative of the total number operator in the system, $\sum_n d_n^\dagger d_n$, which is just $\dot{\boldsymbol{d}}^\dagger \boldsymbol{d} + \boldsymbol{d}^\dagger \dot{\boldsymbol{d}}$ in a matrix form. From Eq. (32), we find that

$$\begin{aligned}
\dot{\boldsymbol{d}}(t) = -i\sqrt{2\pi}\boldsymbol{R}^{-1}(t)\Big[&-\boldsymbol{\Lambda}_M\int_{-\infty}^{t} d\tau e^{-\boldsymbol{\Lambda}_M(t-\tau)}\boldsymbol{R}(\tau)\tilde{\boldsymbol{d}}_{in}(\tau)\\
&+\boldsymbol{R}(t)\tilde{\boldsymbol{d}}_{in}(t)\Big] = -\boldsymbol{M}(t)\cdot\boldsymbol{d}(t) - i\sqrt{2\pi}\tilde{\boldsymbol{d}}_{in}(t), \quad \text{(B1)}
\end{aligned}$$

by noting that $\boldsymbol{M}(t) = \boldsymbol{R}^{-1}(t)\cdot\boldsymbol{\Lambda}_M\cdot\boldsymbol{R}(t)$. Hence, we have

$$\begin{aligned}
\frac{d}{dt}\sum_n d_n^\dagger d_n = &-\boldsymbol{d}^\dagger\cdot(\boldsymbol{M}+\boldsymbol{M}^\dagger)\cdot\boldsymbol{d} - i\sqrt{2\pi}\boldsymbol{d}^\dagger\cdot\tilde{\boldsymbol{d}}_{in}\\
&+i\sqrt{2\pi}\tilde{\boldsymbol{d}}_{in}^\dagger\cdot\boldsymbol{d}. \quad \text{(B2)}
\end{aligned}$$

The right-hand side of the above equation is compensated by $d(\sum_{kv} c_{kv}^\dagger c_{kv})/dt = \sum_v (i\sqrt{2\pi}\tilde{d}_\sigma^\dagger d_{in}^v - i\sqrt{2\pi}d_{in}^{v,\dagger}\tilde{d}_\sigma + 2\Gamma_v d_\sigma^\dagger d_\sigma)$. Charge conservation therefore implies that

$$-\boldsymbol{d}^\dagger\cdot(\boldsymbol{M}+\boldsymbol{M}^\dagger)\cdot\boldsymbol{d} + 2\Gamma_v d_\sigma^\dagger d_\sigma = 0, \quad \text{(B3)}$$

which is true regardless of the PoTER approximation. We conclude that the approximate solution Eq. (32) conserves the total charge.

APPENDIX C: CHARGE CURRENT EXPRESSION IN THE GIOM

In this Appendix, we derive the charge current expression under the GIOM and show that it is given by two types of

rates. Performing the PoTER approximation, we reach simple integral forms for these rates that allow facile calculations. In fact, if we only make the second PoTER approximation, that is we propagate the vibrations without back action of electrons, we reach a closed form expression for the current, which allows extensions beyond results presented in this paper.

We begin with Eq. (21), an exact form for the charge current, and focus on

$$\begin{aligned} C_1(t) &\equiv -\sqrt{2\pi}\,\mathrm{Im}\langle d_{in}^{L,\dagger}(t)\tilde{d}_1(t)\rangle \\ &= 2\pi\,\mathrm{Re}\sum_{nm}\int_{-\infty}^{t} d\tau s_{1n}\tilde{s}_{m1}\langle d_{in}^{L,\dagger}(t)D_1^{\dagger}(t)K_{nm}(t,\tau)d_{in}^{L}(\tau)\rangle \\ &+ 2\pi\,\mathrm{Re}\sum_{nm}\int_{-\infty}^{t} d\tau s_{1n}\tilde{s}_{mN}\langle d_{in}^{L,\dagger}(t)D_1^{\dagger}(t)K_{nm}(t,\tau)d_{in}^{R}(\tau)\rangle, \end{aligned} \tag{C1}$$

with the kernel defined in Eq. (31) and the operator of the system given by Eq. (30). To proceed, we make the second PoTER approximation, which allows us to separate the nuclear and electronic correlation functions. Mixed correlation functions of the left and right lead electrons are zero and we get

$$C_1 = 2\pi\,\mathrm{Re}\sum_{nm}\int_{-\infty}^{t} d\tau s_{1n}\tilde{s}_{m1}\langle d_{in}^{L,\dagger}(t)d_{in}^{L}(\tau)\rangle\langle D_1^{\dagger}(t)K_{nm}(t,\tau)\rangle. \tag{C2}$$

We reorganize the result as

$$C_1 = \mathrm{Re}\sum_{nm} s_{1n}\tilde{s}_{m1}\chi_{nm}^{L}, \tag{C3}$$

where

$$\chi_{nm}^{v} = 2\Gamma_v\int\frac{d\epsilon}{2\pi}n_F^{v}(\epsilon)\int_0^{\infty} d\tau e^{i\epsilon\tau}e^{-\Lambda_n\tau}B_{nm}(\tau), \tag{C4}$$

with

$$B_{nm}(t-\tau) = \left\langle \mathcal{D}_{n,b}^{\dagger}(t)\left[\exp\left(\int_{\tau}^{t}(\dot{\boldsymbol{R}}\boldsymbol{R}^{-1})_{\tau'}d\tau'\right)\right]_{nm}\mathcal{D}_{m,b}(\tau)\right\rangle. \tag{C5}$$

We identify χ_{nm}^{v} as the first-order rate; it depends on a single electronic resonance. The correlation function $B_{nm}(t-\tau)$ only involves vibrational degrees of freedom and one should be able to simulate it under certain assumptions. Here, we perform the PoTER and replace $[\exp(\int_{\tau}^{t}(\dot{\boldsymbol{R}}\boldsymbol{R}^{-1})_{\tau'}d\tau')]_{nm}$ with δ_{nm}. This allows us to reach

$$C_1 = \mathrm{Re}\sum_{n} s_{1n}\tilde{s}_{n1}\chi_n^{L}, \tag{C6}$$

with

$$\chi_n^{v} = 2\Gamma_v\int\frac{d\epsilon}{2\pi}n_F^{v}(\epsilon)\int_0^{\infty} d\tau e^{i\epsilon\tau}e^{-\Lambda_n\tau}\langle\mathcal{D}_{n,b}^{\dagger}(\tau)\mathcal{D}_{n,b}(0)\rangle. \tag{C7}$$

Next, we analyze the second contribution in the charge current expression:

$$C_2 \equiv \langle d_1^{\dagger}d_1\rangle. \tag{C8}$$

We decouple the electronic and vibrational degrees of freedom and get

$$\begin{aligned} C_2 &= 2\pi\sum_{nm}\sum_{n'm'}s_{1n}^{\star}\tilde{s}_{m1}^{\star}s_{1n'}\tilde{s}_{m'1}\int_{-\infty}^{t}d\tau\int_{-\infty}^{t}d\tau'\langle d_{in}^{L,\dagger}(\tau)d_{in}^{L}(\tau')\rangle\langle K_{nm}^{\dagger}(t,\tau)K_{n'm'}(t,\tau')\rangle \\ &+2\pi\sum_{nm}\sum_{n'm'}s_{1n}^{\star}\tilde{s}_{mN}^{\star}s_{1n'}\tilde{s}_{m'N}\int_{-\infty}^{t}d\tau\int_{-\infty}^{t}d\tau'\langle d_{in}^{R,\dagger}(\tau)d_{in}^{R}(\tau')\rangle\langle K_{nm}^{\dagger}(t,\tau)K_{n'm'}(t,\tau')\rangle. \end{aligned} \tag{C9}$$

Using the PoTER kernel, this simplifies to

$$\begin{aligned} C_2 &= 2\pi\sum_{n}\sum_{n'}s_{1n}^{\star}\tilde{s}_{n1}^{\star}s_{1n'}\tilde{s}_{n'1}\int_{-\infty}^{t}d\tau\int_{-\infty}^{t}d\tau'\langle d_{in}^{L,\dagger}(\tau)d_{in}^{L}(\tau')\rangle e^{-\Lambda_n^{\star}(t-\tau)}e^{-\Lambda_{n'}(t-\tau')}\langle\mathcal{D}_{n,b}^{\dagger}(\tau)\mathcal{D}_{n,b}(t)\mathcal{D}_{n',b}^{\dagger}(t)\mathcal{D}_{n',b}(\tau')\rangle \\ &+2\pi\sum_{n}\sum_{n'}s_{1n}^{\star}\tilde{s}_{nN}^{\star}s_{1n'}\tilde{s}_{n'N}\int_{-\infty}^{t}d\tau\int_{-\infty}^{t}d\tau'\langle d_{in}^{R,\dagger}(\tau)d_{in}^{R}(\tau')\rangle e^{-\Lambda_n^{\star}(t-\tau)}e^{-\Lambda_{n'}(t-\tau')}\langle\mathcal{D}_{n,b}^{\dagger}(\tau)\mathcal{D}_{n,b}(t)\mathcal{D}_{n',b}^{\dagger}(t)\mathcal{D}_{n',b}(\tau')\rangle. \end{aligned} \tag{C10}$$

This expression comprises the so-called second-order rate, since two resonances act together to build the transfer rate. Noting that the correlation functions on different sites are uncorrelated, we recover Eqs. (39) and (40) in the main text.

APPENDIX D: EVALUATION OF VIBRATIONAL CORRELATION FUNCTIONS

In this Appendix, we calculate the polaron correlation function:

$$B_n(t,t') = \langle\mathcal{D}_{n,b}^{\dagger}(t)\mathcal{D}_{n,b}(t')\rangle. \tag{D1}$$

Recall that the primary vibrations are coupled to a secondary phonon bath, leading to level broadening ν_n.

We begin with the correlation function of displacement operators. For the sake of simplicity, we omit the subscript n. Neglecting the back action of electrons, the GIOM HLE for the vibrations satisfy

$$\dot{b} = -(\nu + i\omega_b)b - i\sqrt{2\pi}b_{in}. \tag{D2}$$

The formal solution of b, together with Eq. (A1a) lead to the commutation relation

$$[b(t), b^\dagger(t')] = \int d\omega \frac{\nu(\omega)}{\pi} \frac{e^{-i\omega(t-t')}}{\nu^2 + (\omega - \omega_b)^2}. \tag{D3}$$

Considering a two-time correlation function $B(t,t') = \langle \mathcal{D}_b^\dagger(t)\mathcal{D}_b(t')\rangle$, we have

$$B(t,t') = \exp\left[-\lambda^2 \int d\omega \frac{\nu(\omega)}{\pi} \frac{1 - e^{-i\omega(t-t')}}{\nu^2 + (\omega - \omega_b)^2}\right] \times \underbrace{\langle e^{-\lambda b^\dagger(t)} e^{\lambda b^\dagger(t')} e^{\lambda b(t)} e^{-\lambda b(t')}\rangle}_{C(t,t')}. \tag{D4}$$

The ensemble average of $C(t,t')$ is performed with respect to the thermal equilibrium state of the thermal bath.

Adopting the technique of Feynman disentangling of operators [130] and the formal definition of the input field $b_{in}(t)$, we find

$$C(t,t') = \exp\left[-\sum_j \frac{|\mu_j(t,t')|^2}{e^{\beta\omega_j} - 1}\right] \tag{D5}$$

with $\mu_j(t,t') = -i\lambda\gamma_j \frac{e^{i\omega_j(t-t_0)} - e^{i\omega_j(t'-t_0)}}{\nu - i\omega_b + i\omega_j}$. Inserting $C(t,t')$ into $B(t,t')$, we recover Eq. (38) in the main text.

[1] J. C. Cuevas and E. Scheer, *Molecular Electronics: An Introduction To Theory And Experiment* (World Scientific, Singapore, 2010).

[2] A. Aviram and M. A. Ratner, Molecular rectifiers, Chem. Phys. Lett. **29**, 277 (1974).

[3] D. J. Wold and C. D. Frisbie, Fabrication and characterization of metal-molecule-metal junctions by conducting probe atomic force microscopy, J. Am. Chem. Soc. **123**, 5549 (2001).

[4] R. E. Holmlin, R. Haag, M. L. Chabinyc, R. F. Ismagilov, A. E. Cohen, A. Terfort, M. Rampi, and G. M. Whitesides, Electron transport through thin organic films in metal-insulator-metal junctions based on self-assembled monolayers, J. Am. Chem. Soc. **123**, 5075 (2001).

[5] N. B. Zhitenev, H. Meng, and Z. Bao, Conductance of Small Molecular Junctions, Phys. Rev. Lett. **88**, 226801 (2002).

[6] N. Agrait, A. Yeyati, and J. M. van Ruitenbeek, Quantum properties of atomic-sized conductors, Phys. Rep. **377**, 81 (2003).

[7] N. Tao, Electron transport in molecular junctions, Nat. Nanotech. **1**, 173 (2006).

[8] L. Venkataraman, J. E. Klare, C. Nuckolls, M. S. Hybertsen, and M. L. Steigerwald, Dependence of single-molecule junction conductance on molecular conformation, Nature **442**, 904 (2006).

[9] D. Ward, G. Scott, Z. Keane, N. Halas, and D. Natelson, Electronic and optical properties of electromigrated molecular junctions, J. Phys.: Condens. Matter **20**, 374118 (2008).

[10] R. L. McCreery and A. J. Bergren, Progress with molecular electronic junctions: Meeting experimental challenges in design and fabrication, Adv. Mater. **21**, 4303 (2009).

[11] K. Moth-Poulsen and T. Bjornholm, Molecular electronics with single molecules in solid-state devices, Nat. Nanotech. **4**, 551 (2009).

[12] N. Tuccitto, V. Ferri, M. Cavazzini, S. Quici, G. Zhavnerko, A. Licciardello, and M. A. Rampi, Highly conductive 40-nm-long molecular wires assembled by stepwise incorporation of metal centres, Nat. Mater. **8**, 41 (2008).

[13] L. Lafferentz, F. Ample, H. Yu, S. Hecht, C. Joachim, and L. Grill, Conductance of a single conjugated polymer as a continuous function of its length, Science **323**, 1193 (2009).

[14] S. V. Aradhya and L. Venkataraman, Single-molecule junctions beyond electronic transport, Nat. Nanotech. **8**, 399 (2013).

[15] D. Xiang, X. Wang, C. Jia, T. Lee, and X. Guo, Molecular-scale electronics: From concept to function, Chem. Rev. **116**, 4318 (2016).

[16] H. B. Akkerman and B. de Boer, Electrical conduction through single molecules and self-assembled monolayers, J. Phys.: Condens. Matter **20**, 013001 (2007).

[17] T. A. Su, M. Neupane, M. L. Steigerwald, L. Venkataraman, and C. Nuckolls, Chemical principles of single-molecule electronics, Nat. Rev. Mater. **1**, 16002 (2016).

[18] L. Cui, R. Miao, C. Jiang, E. Meyhofer, and P. Reddy, Perspective: Thermal and thermoelectric transport in molecular junctions, J. Chem. Phys. **146**, 092201 (2017).

[19] M. Thoss and F. Evers, Perspective: Theory of quantum transport in molecular junctions, J. Chem. Phys. **148**, 030901 (2018).

[20] Y. Selzer, M. A. Cabassi, T. S. Mayer, and D. L. Allara, Thermally activated conduction in molecular junctions, J. Am. Chem. Soc. **126**, 4052 (2004).

[21] Y. Selzer, M. A. Cabassi, T. S. Mayer, and D. L. Allara, Temperature effects on conduction through a molecular junction, Nanotechnology **15**, S483 (2004).

[22] E. A. Weiss, M. J. Tauber, R. F. Kelley, M. J. Ahrens, M. A. Ratner, and M. R. Wasielewski, Conformationally gated switching between superexchange and hopping within oligo-*p*-phenylene-based molecular wires, J. Am. Chem. Soc. **127**, 11842 (2005).

[23] Y. Selzer and D. L. Allara, Single-molecule electrical junctions, Annu. Rev. Phys. Chem. **57**, 593 (2006).

[24] M. Poot, E. Osorio, K. O'Neill, J. M. Thijssen, D. Vanmaekelbergh, C. A. van Walree, L. W. Jenneskens, and H. S. J. van der Zant, Temperature dependence of three-terminal molecular junctions with sulfur end-functionalized tercyclohexylidenes, Nano Lett. **6**, 1031 (2006).

[25] R. H. Goldsmith, O. DeLeon, T. M. Wilson, D. Finkelstein-Shapiro, M. A. Ratner, and M. R. Wasielewski, Challenges in distinguishing superexchange and hopping mechanisms of intramolecular charge transfer through fluorene oligomers, J. Phys. Chem. A **112**, 4410 (2008).

[26] S. Ho Choi, B. Kim, and C. D. Frisbie, Electrical resistance of long conjugated molecular wires, Science **320**, 1482 (2008).

[27] Q. Lu, K. Liu, H. Zhang, Z. Du, X. Wang, and F. Wang, From tunneling to hopping: A comprehensive investigation of charge transport mechanism in molecular junctions based on oligo(p-phenylene ethynylene)s, ACS Nano **3**, 3861 (2009).

[28] L. Luo and C. D. Frisbie, Length-dependent conductance of conjugated molecular wires synthesized by stepwise "click" chemistry, J. Am. Chem. Soc., **132**, 8854 (2010).

[29] S. Choi, C. Risko, M. Delgado, B. Kim, J. Brédas, and C. D. Frisbie, Transition from tunneling to hopping transport in long, conjugated oligo-imine wires connected to metals, J. Am. Chem. Soc. **132**, 4358 (2010).

[30] T. Hines, I. Diez-Perez, J. Hihath, H. Liu, Z. Wang, J. Zhao, G. Zhou, K. Müllen, and N. Tao, Transition from tunneling to hopping in single molecular junctions by measuring length and temperature dependence, J. Am. Chem. Soc. **132**, 11658 (2010).

[31] L. Luo, S. Choi, and C. D. Frisbie, Probing hopping conduction in conjugated molecular wires connected to metal electrodes, Chem. Mater. **23**, 631 (2011).

[32] G. Sedghi, V. García-Suárez, L. J. Esdaile, H. L. Anderson, C. J. Lambert, S. Martín, D. Bethell, S. J. Higgins, M. Elliott, N. Bennett, J. E. Macdonald, and R. J. Nichols, Long-range electron tunneling in oligo-porphyrin molecular wires, Nat. Nanotech. **6**, 517 (2011).

[33] Z. Li, T. Park, J. Rawson, M. J. Therien, and E. Borguet, Quasi-ohmic single molecule charge transport through highly conjugated meso-to-meso ethyne-bridged porphyrin wires, Nano Lett. **12**, 2722 (2012).

[34] D. Taherinia, C. E. Smith, S. Ghosh, S. O. Odoh, L. Balhorn, L. Gagliardi, C. J. Cramer, and C. D. Frisbie, Charge transport in 4 nm molecular wires with interrupted conjugation: Combined experimental and computational evidence for thermally assisted polaron tunneling, ACS Nano **10**, 4372 (2016).

[35] J. O. Thomas, B. Limburg, J. K. Sowa, K. Willick, J. Baugh, G. A. D. Briggs, E. M. Gauger, H. L. Anderson, and J. A. Mol, Understanding resonant charge transport through weakly coupled single-molecule junctions, Nat. Commun. **10**, 4628 (2019).

[36] G. C. Solomon, C. Herrmann, T. Hansen, V. Mujica, and M. A. Ratner, Exploring local currents in molecular junctions, Nat. Chem. **2**, 223 (2010).

[37] C. M. Guédon, H. Valkenier, T. Markussen, K. S. Thygesen, J. C. Hummelen, and S. J. van der Molen, Observation of quantum interference in molecular charge transport, Nat. Nanotech. **7**, 305 (2012).

[38] H. Vazquez, R. Skouta, S. Schneebeli, M. Kamenetska, R. Breslow, L. Venkataraman, and M. S. Hybertsen, Probing the conductance superposition law in single-molecule circuits with parallel paths, Nat Nanotech. **7**, 663 (2012).

[39] M. H. Garner, H. Li, Y. Chen, T. A. Su, Z. Shangguan, D. W. Paley, T. Liu, F. Ng, H. Li, S. Xiao, C. Nuckolls, L. Venkataraman, and G. C. Solomon, Comprehensive suppression of single-molecule conductance using destructive σ-interference, Nature **558**, 415 (2018).

[40] F. Evers, R. Korytár, S. Tewari, and J. M. van Ruitenbeek, Advances and challenges in single-molecule electron transport, arXiv:1906.10449.

[41] P. Reddy, S. Jang, R. A. Segalman, and A. Majumdar, Thermoelectricity in molecular junctions, Science **315**, 1568 (2007).

[42] J. A. Malen, P. Doak, K. Baheti, T. D. Tilley, R. A. Segalman, and A. Majumdar, Identifying the length dependence of orbital alignment and contact coupling in molecular heterojunctions, Nano Lett. **9**, 1164 (2009).

[43] N. A. Zimbovskaya, Communication: Length-dependent thermopower of single-molecule junctions, J. Chem. Phys. **145**, 221101 (2016).

[44] L. Rincón-García, C. Evangeli, G. Rubio-Bollinger, and N. Agraït, Thermopower measurements in molecular junctions, Chem. Soc. Rev. **45**, 4285 (2016).

[45] S. Schmaus, A. Bagrets, Y. Nahas, T. K. Yamada, A. Bork, M. Bowen, E. Beaurepaire, F. Evers, and W. Wulfhekel, Giant magnetoresistance through a single molecule, Nat. Nanotech. **6**, 185 (2011).

[46] W. Liang, M. P. Shores, M. Bockrath, J. R. Long, and H. Park, Kondo resonance in a single-molecule transistor, Nature **417**, 725 (2002).

[47] G. Scott and D. Natelson, Kondo resonances in molecular devices, ACS Nano **4**, 3560 (2010).

[48] B. Göhler, V. Hamelbeck, T. Z. Markus, M. Kettner, G. F. Hanne, Z. Vager, R. Naaman, and H. Zacharias, Spin selectivity in electron transmission through self-assembled monolayers of double-stranded DNA, Science **331**, 894 (2011).

[49] R. Naaman and D. H. Waldeck, Spintronics and chirality: Spin selectivity in electron transport through chiral molecules, Ann. Rev. Phys. Chem. **66**, 263 (2015).

[50] R. Naaman, Y. Paltiel, and D. H. Waldeck, Chiral molecules and the electron spin, Nat. Rev. Chem. **3**, 250 (2019).

[51] J. Koch and F. von Oppen, Franck-Condon Blockade and Giant Fano Factors in Transport through Single Molecules, Phys. Rev. Lett. **94**, 206804 (2005).

[52] J. Koch, F. von Oppen, and A. V. Andreev, Theory of the Franck-Condon blockade regime, Phys. Rev. B **74**, 205438 (2006).

[53] R. Leturcq, C. Stampfer, K. Inderbitzin, L. Durrer, C. Hierold, E. Mariani, M. G. Schultz, F. von Oppen, and K. Ensslin, Franck-condon blockade in suspended carbon nanotube quantum dots, Nat. Phys. **5**, 327 (2009).

[54] E. Burzurí, Y. Yamamoto, M. Warnock, X. Zhong, K. Park, A. Cornia, and H. S. J. van der Zant, Franck-Condon blockade in a single-molecule transistor, Nano Lett. **14**, 3191 (2014).

[55] C. Lau, H. Sadeghi, G. Rogers, S. Sangtarash, P. Dallas, K. Porfyrakis, J. Warner, C. J. Lambert, G. A. D. Briggs, and J. A. Mol, Redox-dependent Franck-Condon blockade and avalanche transport in a graphene-fullerene single-molecule transistor, Nano Lett. **16**, 170 (2016).

[56] H. Ness, S. A. Shevlin, and A. J. Fisher, Coherent electron-phonon coupling and polaronlike transport in molecular wires, Phys. Rev. B **63**, 125422 (2001).

[57] M. Čížek, M. Thoss, and W. Domcke, Theory of vibrationally inelastic electron transport through molecular bridges, Phys. Rev. B **70**, 125406 (2004).

[58] M. Caspary Toroker and U. Peskin, Electronic transport through molecular junctions with nonrigid molecule-leads coupling, J. Chem. Phys. **127**, 154706 (2007).

[59] C. Benesch, M. Cizek, J. Klimes, I. Kondov, M. Thoss, and W. Domcke, Vibronic effects in single molecule conductance: First-principles description and application to benzenealkanethiolates between gold electrodes, J. Phys. Chem. C **112**, 9880 (2008).

[60] N. A. Zimbovskaya and M. M. Kuklja, Vibration-induced inelastic effects in the electron transport through multisite molecular bridges, J. Chem. Phys. **131**, 114703 (2009).

[61] R. Jorn and T. Seideman, Competition between current-induced excitation and bath-induced decoherence in molecular junctions, J. Chem. Phys. **131**, 244114 (2009).

[62] J. Koch, M. Semmelhack, F. von Oppen, and A. Nitzan, Current-induced nonequilibrium vibrations in single-molecule devices, Phys. Rev. B **73**, 155306 (2006).

[63] X. Y. Shen, Bing Dong, X. L. Lei, and N. J. M. Horing, Vibration-mediated resonant tunneling and shot noise through a molecular quantum dot, Phys. Rev. B **76**, 115308 (2007).

[64] A. A. Dzhioev and D. S. Kosov, Kramers problem for nonequilibrium current-induced chemical reactions, J. Chem. Phys. **135**, 074701 (2011).

[65] B. Li, E. Y. Wilner, M. Thoss, E. Rabani, and W. H. Miller, A quasi-classical mapping approach to vibrationally coupled electron transport in molecular junctions, J. Chem. Phys. **140**, 104110 (2014).

[66] D. Segal, A. Nitzan, W. B. Davis, M. R. Wasielewski, and M. A. Ratner, Electron transfer rates in bridged molecular systems 2. A steady-state analysis of coherent tunneling and thermal transitions, J. Phys. Chem. B **104**, 3817 (2000).

[67] V. May, Electron transfer through a molecular wire: Consideration of electron-vibrational coupling within the Liouville space pathway technique, Phys. Rev. B **66**, 245411 (2002).

[68] A. Mitra, I. Aleiner, and A. J. Millis, Phonon effects in molecular transistors: Quantal and classical treatment, Phys. Rev. B **69**, 245302 (2004).

[69] J. N. Pedersen and A. Wacker, Tunneling through nanosystems: Combining broadening with many-particle states, Phys. Rev. B **72**, 195330 (2005).

[70] U. Harbola, M. Esposito, and S. Mukamel, Quantum master equation for electron transport through quantum dots and single molecules, Phys. Rev. B **74**, 235309 (2006).

[71] A. Donarini, M. Grifoni, and K. Richter, Dynamical Symmetry Breaking in Transport Through Molecules, Phys. Rev. Lett. **97**, 166801 (2006).

[72] M. Leijnse and M. R. Wegewijs, Kinetic equations for transport through single-molecule transistors, Phys. Rev. B **78**, 235424 (2008).

[73] C. Timm, Tunneling through molecules and quantum dots: Master-equation approaches, Phys. Rev. B **77**, 195416 (2008).

[74] M. Esposito and M. Galperin, Transport in molecular states language: Generalized quantum master equation approach, Phys. Rev. B **79**, 205303 (2009).

[75] R. Volkovich, R. Härtle, M. Thoss, and U. Peskin, Bias-controlled selective excitation of vibrational modes in molecular junctions: A route towards mode-selective chemistry, Phys. Chem. Chem. Phys. **13**, 14333 (2011).

[76] R. Härtle and M. Thoss, Resonant electron transport in single-molecule junctions: Vibrational excitation, rectification, negative differential resistance, and local cooling, Phys. Rev. B **83**, 115414 (2011).

[77] J. K. Sowa, J. A. Mol, G. A. D. Briggs, and E. M. Gauger, Environment-assisted quantum transport through single-molecule junctions, Phys. Chem. Chem. Phys. **19**, 29534 (2017).

[78] K. Flensberg, Tunneling broadening of vibrational sidebands in molecular transistors, Phys. Rev. B **68**, 205323 (2003).

[79] M. Galperin, M. A. Ratner, and A. Nitzan, Inelastic electron tunneling spectroscopy in molecular junctions: Peaks and dips, J. Chem. Phys. **121**, 11965 (2004).

[80] M. Galperin, A. Nitzan, and M. A. Ratner, Resonant inelastic tunneling in molecular junctions, Phys. Rev. B **73**, 045314 (2006).

[81] M. Galperin, A. Nitzan, and M. A. Ratner, Inelastic tunneling effects on noise properties of molecular junctions, Phys. Rev. B **74**, 075326 (2006).

[82] D. A. Ryndyk, M. Hartung, and G. Cuniberti, Nonequilibrium molecular vibrons: An approach based on the nonequilibrium green function technique and the self-consistent born approximation, Phys. Rev. B **73**, 045420 (2006).

[83] T. Frederiksen, M. Paulsson, M. Brandbyge, and A.-P. Jauho, Inelastic transport theory from first principles: Methodology and application to nanoscale devices, Phys. Rev. B **75**, 205413 (2007).

[84] O. Entin-Wohlman, Y. Imry, and A. Aharony, Voltage-induced singularities in transport through molecular junctions, Phys. Rev. B **80**, 035417 (2009).

[85] R. Härtle, C. Benesch, and M. Thoss, Multimode vibrational effects in single-molecule conductance: A nonequilibrium Green's function approach, Phys. Rev. B **77**, 205314 (2008).

[86] R. Härtle, C. Benesch, and M. Thoss, Vibrational Nonequilibrium Effects in the Conductance of Single Molecules with Multiple Electronic States, Phys. Rev. Lett. **102**, 146801 (2009).

[87] A. Erpenbeck, R. Härtle, and M. Thoss, Effect of nonadiabatic electronic-vibrational interactions on the transport properties of single-molecule junctions, Phys. Rev. B **91**, 195418 (2015).

[88] G. Cabra, A. Jensen, and M. Galperin, On simulation of local fluxes in molecular junctions, J. Chem. Phys. **148**, 204103 (2018).

[89] M. Galperin, M. A. Ratner, and A. Nitzan, Molecular transport junctions: Vibrational effects, J. Phys.: Condens. Matter **19**, 103201 (2007).

[90] J. Jin, X. Zheng, and Y. Yan, Exact dynamics of dissipative electronic systems and quantum transport: Hierarchical equations of motion approach, J. Chem. Phys. **128**, 234703 (2008).

[91] Z. H. Li, N. H. Tong, X. Zheng, D. Hou, J. H. Wei, J. Hu, and Y. J. Yan, Hierarchical Liouville-Space Approach for Accurate and Universal Characterization of Quantum Impuritysystems, Phys. Rev. Lett. **109**, 266403 (2012).

[92] F. Jiang, J. Jin, S. Wang, and Y. J. Yan, Inelastic electron transport through mesoscopic systems: Heating versus cooling and sequential tunneling versus cotunneling processes, Phys. Rev. B **85**, 245427 (2012).

[93] R. Härtle, G. Cohen, D. R. Reichman, and A. J. Millis, Decoherence and lead-induced interdot coupling in nonequilibrium electron transport through interacting quantum dots: A hierarchical quantum master equation approach, Phys. Rev. B **88**, 235426 (2013).

[94] R. Härtle and A. J. Millis, Formation of nonequilibrium steady states in interacting double quantum dots: When coherences dominate the charge distribution, Phys. Rev. B **90**, 245426 (2014).

[95] R. Härtle, G. Cohen, D. R. Reichman, and A. J. Millis, Transport through an anderson impurity: Current ringing, nonlinear magnetization, and a direct comparison of continuous-time quantum monte carlo and hierarchical quantum master equations, Phys. Rev. B **92**, 085430 (2015).

[96] C. Schinabeck, A. Erpenbeck, R. Härtle, and M. Thoss, Hierarchical quantum master equation approach to electronic-

vibrational coupling in nonequilibrium transport through nanosystems, Phys. Rev. B **94**, 201407(R) (2016).

[97] C. Schinabeck, R. Härtle, and M. Thoss, Hierarchical quantum master equation approach to electronic-vibrational coupling in nonequilibrium transport through nanosystems: Reservoir formulation and application to vibrational instabilities, Phys. Rev. B **97**, 235429 (2018).

[98] A. Erpenbeck, C. Hertlein, C. Schinabeck, and M. Thoss, Extending the hierarchical quantum master equation approach to low temperatures and realistic band structures, J. Chem. Phys. **149**, 064106 (2018).

[99] E. Y. Wilner, H. Wang, M. Thoss, and E. Rabani, Nonequilibrium quantum systems with electron-phonon interactions: Transient dynamics and approach to steady state, Phys. Rev. B **89**, 205129 (2014).

[100] H. Wang and M. Thoss, Numerically exact quantum dynamics for indistinguishable particles: The multilayer multiconfiguration time-dependent Hartree theory in second quantization representation, J. Chem. Phys. **131**, 024114 (2009).

[101] P. Werner, T. Oka, and A. J. Millis, Diagrammatic monte carlo simulation of nonequilibrium systems, Phys. Rev. B **79**, 035320 (2009).

[102] E. Gull, A. J. Millis, A. I. Lichtenstein, A. N. Rubtsov, M. Troyer, and P. Werner, Continuous-time Monte Carlo methods for quantum impurity models, Rev. Mod. Phys. **83**, 349 (2011).

[103] G. Cohen, E. Gull, D. R. Reichman, A. J. Millis, and E. Rabani, Numerically exact long-time magnetization dynamics at the nonequilibrium kondo crossover of the Anderson impurity model, Phys. Rev. B **87**, 195108 (2013).

[104] L. Mühlbacher and E. Rabani, Real-Time Path Integral Approach to Nonequilibrium Many-Body Quantum Systems, Phys. Rev. Lett. **100**, 176403 (2008).

[105] S. Weiss, J. Eckel, M. Thorwart, and R. Egger, Iterative real-time path integral approach to nonequilibrium quantum transport, Phys. Rev. B **77**, 195316 (2008).

[106] D. Segal, A. J. Millis, and D. R. Reichman, Numerically exact path-integral simulation of nonequilibrium quantum transport and dissipation, Phys. Rev. B **82**, 205323 (2010).

[107] P. E. Kornilovitch, A. M. Bratkovsky, and R. S. Williams, Current rectification by molecules with asymmetric tunneling barriers, Phys. Rev. B **66**, 165436 (2002).

[108] C. Verdozzi, G. Stefanucci, and C. O. Almbladh, Classical Nuclear Motion in Quantum Transport, Phys. Rev. Lett. **97**, 046603 (2006).

[109] A. Arnold, F. Weigend, and F. Evers, Quantum chemistry calculations for molecules coupled to reservoirs: Formalism, implementation, and application to benzenedithiol, J. Chem. Phys. **126**, 174101 (2007).

[110] M. J. Collett and C. W. Gardiner, Squeezing of intracavity and traveling-wave light fields produced in parametric amplification, Phys. Rev. A **30**, 1386 (1984).

[111] C. W. Gardiner and M. J. Collett, Input and output in damped quantum systems: Quantum stochastic differential equations and the master equation, Phys. Rev. A **31**, 3761 (1985).

[112] C. P. Search, S. Pötting, W. Zhang, and P. Meystre, Input-output theory for fermions in an atom cavity, Phys. Rev. A **66**, 043616 (2002).

[113] C. W. Gardiner and P. Zoller, *Quantum Noise: A Handbook of Markovian and Non-Markovian Quantum Stochastic Methods with Applications to Quantum Optics* (Springer, Berlin, 2004).

[114] C. Ciuti and I. Carusotto, Input-output theory of cavities in the ultrastrong coupling regime: The case of time-independent cavity parameters, Phys. Rev. A **74**, 033811 (2006).

[115] C. Genes, D. Vitali, P. Tombesi, S. Gigan, and M. Aspelmeyer, Ground-state cooling of a micromechanical oscillator: Comparing cold damping and cavity-assisted cooling schemes, Phys. Rev. A **77**, 033804 (2008).

[116] A. A. Clerk, M. H. Devoret, S. M. Girvin, F. Marquardt, and R. J. Schoelkopf, Introduction to quantum noise, measurement, and amplification, Rev. Mod. Phys. **82**, 1155 (2010).

[117] P. Rabl, Photon Blockade Effect in Optomechanical Systems, Phys. Rev. Lett. **107**, 063601 (2011).

[118] A. Nunnenkamp, K. Børkje, and S. M. Girvin, Single-Photon Optomechanics, Phys. Rev. Lett. **107**, 063602 (2011).

[119] M. Reitz, C. Sommer, and C. Genes, Langevin Approach to Quantum Optics with Molecules, Phys. Rev. Lett. **122**, 203602 (2019).

[120] A. H. Kiilerich and K. Mølmer, Input-Output Theory with Quantum Pulses, Phys. Rev. Lett. **123**, 123604 (2019).

[121] J. Liu and D. Segal, Generalized input-output method to quantum transport junctions. II. Applications, Phys. Rev. B **101**, 155407 (2020).

[122] J. K. Sowa, J. A. Mol, G. A. D. Briggs, and E. M. Gauger, Vibrational effects in charge transport through a molecular double quantum dot, Phys. Rev. B **95**, 085423 (2017).

[123] M. J. Gullans, Y.-Y. Liu, J. Stehlik, J. R. Petta, and J. M. Taylor, Phonon-Assisted Gain in a Semiconductor Double Quantum Dot Maser, Phys. Rev. Lett. **114**, 196802 (2015).

[124] N. S. Wingreen, K. W. Jacobsen, and J. W. Wilkins, Inelastic scattering in resonant tunneling, Phys. Rev. B **40**, 11834 (1989).

[125] G. E. Topp, T. Brandes, and G. Schaller, Steady-state thermodynamics of non-interacting transport beyond weak coupling, Europhys. Lett. **110**, 67003 (2015).

[126] E. Jussiau, M. Hasegawa, and R. S. Whitney, Signature of the transition to a bound state in thermoelectric quantum transport, Phys. Rev. B **100**, 115411 (2019).

[127] P. Y. Yang, C. Y. Lin, and W. M. Zhang, Master equation approach to transient quantum transport in nanostructures incorporating initial correlations, Phys. Rev. B **92**, 165403 (2015).

[128] S. Maier, T. L. Schmidt, and A. Komnik, Charge transfer statistics of a molecular quantum dot with strong electron-phonon interaction, Phys. Rev. B **83**, 085401 (2011).

[129] R. Seoane Souto, R. Avriller, R. C. Monreal, A. Martín-Rodero, and A. Levy Yeyati, Transient dynamics and waiting time distribution of molecular junctions in the polaronic regime, Phys. Rev. B **92**, 125435 (2015).

[130] G. D. Mahan, *Many-Particle Physics* (Plenum, New York, 2000).